

Interpolative Approach for Solving Quantum Impurity Model Based on the Slave–Boson Mean–Field Approximation

V. Oudovenko^{a,e}, K. Haule^{b,e}, S. Y. Savrasov^c, D. Villani^{d,e}, G. Kotliar^e

^aLaboratory for Theoretical Physics, Joint Institute for Nuclear Research, 141980 Dubna, Russia

^bJožef Stefan Institute, SI-1000 Ljubljana, Slovenia

^cDepartment of Physics, New Jersey Institute of Technology, Newark, NJ 07102, USA

^dHess Energy Trading Company, LLC, New York, NY 10036, USA and

^eDepartment of Physics and Center for Material Theory, Rutgers University, Piscataway, NJ 08854, USA

(Dated: November 13, 2018)

A rational representation for the self-energy is explored to interpolate the solution of the Anderson impurity model in general orbitally degenerate case. Several constrains such as the Friedel's sum rule, high-frequency moments and the value of quasiparticle residue are used to establish the equations for the coefficients of the interpolation. We test two fast techniques, the slave–boson mean–field and the Hubbard I approximation to determine the coefficients. The obtained self–energies are compared with the results of numerically exact Quantum Monte Carlo method. We find that using the slave–boson mean–field approach we can construct an accurate self–energy for all frequencies via the proposed interpolation procedure.

PACS numbers: 71.10.-w, 71.27.+a, 71.30.+h

I. INTRODUCTION

There has been recent progress in understanding physics of strongly correlated electronic systems and their electronic structure near a localization–delocalization transition through the development of dynamical mean–field theory (DMFT)¹. Merging this computationally tractable many–body technique with realistic local–density–approximation (LDA)² based electronic structure calculations of strongly correlated solids is promising due to its simplicity and correctness in both band and atomic limits. At present, much effort is being made in this direction including the developments of a LDA+DMFT method³, LDA++ approach⁴, combined GW and DMFT theory⁵ as well as applications to various systems such as $\text{La}_{1-x}\text{Sr}_x\text{TiO}_3$ ⁶, V_2O_3 ⁷, Fe and Ni⁸, Ce⁹, Pu^{10,11}, and many others. For a review, see Ref. 12.

The development of *ab initio* DMFT scheme requires fast methods and algorithms to solve the Anderson impurity model¹³ in general multiorbital case. Present techniques based on either non–crossing approximation (NCA) or iterative perturbation theory (IPT) are unable to provide the solution to that problem due to a limited number of regimes where these methods can be applied¹. The Quantum Monte Carlo (QMC) technique^{1,14} is very accurate and can cope with multiorbital situation but not with multiplet interactions. Also its applicability so far has been limited either to a small number of orbitals or to unphysically large temperatures due to its computational cost. Recently some progress has been achieved using impurity solvers that improve upon the NCA approximation^{15,16,17}, but it has not been possible to retrieve Fermi liquid behavior at very low temperatures with these methods in the orbitally degenerate case.

In this paper we explore the possibility to use interpo-

lation for the self–energy of the quantum impurity model in general multiorbital situation. We do not attempt to develop an alternative method for solving the impurity problem, but follow the ideology of LDA theory where approximations were designed by analytical fits¹⁸ to the Quantum Monte Carlo simulations for homogeneous electron gas¹⁹. Numerically very expensive QMC calculations for the impurity model display smooth self–energies at imaginary frequencies for a wide range of interactions and dopings, and it is therefore tempting to design such an interpolation. We also keep in mind that for many applications a high precision in reproducing the self–energies may not be required. One of such applications is, for example, the calculation of the total energy^{9,10,11} which, as well known from LDA based experience, may not be so sensitive to the details of the one–electron spectra. As a result, we expect that even crude evaluations of the self–energy shapes on imaginary frequency axis may be sufficient for solving many realistic total energy problems. Another point is a computational efficiency. Bringing full self–consistent loops with respect to charge densities¹⁰ and other spectral functions require many iterations towards the convergency which may not need too accurate frequency resolutions at every step. This view should, of course, be contrasted with calculation of properties such as the low–energy spectroscopy and especially transport where delicate distribution of spectral weight at low energy, namely the imaginary part of the analytically continued self–energy, needs to be computed with much greater precision. Here, extensions of the interpolative algorithms should be implemented and its beyond the scope of the present work.

We can achieve a fast interpolative algortihm for the self–energy utilizing a rational representation. The coefficients in this interpolation can be found by forcing the self–energy to obey several limits and constrains. For example, if infinite frequency (Hartree–Fock) limit, high–

frequency moments of the self-energy, low-frequency mass renormalization, number of particles as well as the value of the self-energy at zero frequency are known from independent calculation, the set of interpolating coefficients is well defined. In this work, we explore the slave-boson Gutzwiller approach^{20,21,22,23} and the Hubbard I approximation²⁴ to determine these coefficients. Comparing interpolating results with more accurate calculations using the Quantum Monte Carlo method we find that the slave-boson approach predicts the parameters of interpolation with a good accuracy while the Hubbard I method fails in a number of regimes. Thus, interpolation for the self-energy at all frequencies can be obtained from the method designed to work exclusively at low-frequency limit.

Our paper is organized as follows. In Section II we discuss rational interpolation for the self-energy and list the constraints. In Section III we discuss methods for solving Anderson impurity model based on the slave-boson Gutzwiller and the Hubbard I approximations which can be used to find these constraints. We also present our numerical comparisons with the QMC data between various quantities such as the number of particles and the quasiparticle residue. In Section IV we discuss the interpolational approach and compare the self-energies and the Green functions with the QMC results. Section V is the conclusion.

II. INTERPOLATIVE APPROACH

To be specific, we concentrate on the Anderson impurity Hamiltonian

$$H = \sum_{\alpha=1}^N \epsilon_{f\alpha} f_{\alpha}^+ f_{\alpha} + \frac{1}{2} \sum_{\alpha\beta}^N U_{\alpha\beta} n_{\alpha}^f n_{\beta}^f + \sum_{\mathbf{k}\alpha} E_{\mathbf{k}\alpha} c_{\mathbf{k}\alpha}^+ c_{\mathbf{k}\alpha} + \sum_{\mathbf{k}\alpha} [V_{\alpha}^*(\mathbf{k}) f_{\alpha}^+ c_{\mathbf{k}\alpha} + V_{\alpha}(\mathbf{k}) c_{\mathbf{k}\alpha}^+ f_{\alpha}], \quad (1)$$

describing the interaction of the impurity levels $\epsilon_{f\alpha}$ with bands of conduction electrons $E_{\mathbf{k}\alpha}$ via hybridization $V_{\alpha}(\mathbf{k})$. $U_{\alpha\beta}$ is the Coulomb repulsion between different orbitals in the f -band. Inspired by the success of the iterative perturbation theory¹, in order to solve the Anderson impurity model in general multiorbital case, we use a rational interpolative formula for the self-energy. This can be either encoded into a simple form of pole expansion

$$\Sigma_{\alpha}(i\omega) = \Sigma_{\alpha}(i\infty) + \sum_n \frac{W_n^{\alpha}}{i\omega - P_n^{\alpha}}, \quad (2)$$

or, alternatively, in a form of continuous fraction expansion

$$\Sigma_{\alpha}(i\omega) = \Sigma_{\alpha}(i\infty) + \frac{A_{\alpha}}{i\omega - B_{\alpha} - \frac{C_{\alpha}}{i\omega - D_{\alpha}} \dots} \quad (3)$$

The coefficients W_n^{α} , P_n^{α} , in Eq. (2) or the coefficients A_{α} , B_{α} , C_{α} , ... in Eq. (3) are to be determined together with the Hartree Fock value of the self-energy $\Sigma_{\alpha}(i\infty)$. In principle, both representations are equivalent and there is a well-defined non-linear relationship between the parameters entering (2) and (3).

Our basic assumption is that only a few poles in the rational representation (2) or a few coefficients in continuous fraction expansion (3) is necessary to reproduce an overall frequency dependence of the self-energy necessary for the accuracies of the total energy calculations. Extensive experience gained from solving Hubbard and periodic Anderson model within DMFT at various ratios of the on-site Coulomb interaction U to the bandwidth W shows the appearance of lower and upper Hubbard bands as well as renormalized quasiparticle peak in the spectrum of one-electron excitations¹. To describe such three-peak structure we expect that either two- or at most three-pole formulae for the self-energy will suffice. Thus, four (six) unknown parameters need to be determined when using two (three) pole interpolating formulae.

In order to fix the coefficients we can explore several constraints for the self-energy:

a) *Hartree-Fock value.* In the limit $i\omega \rightarrow i\infty$ the self-energy takes its Hartree-Fock form

$$\Sigma_{\alpha}(i\infty) = \sum_{\beta} U_{\alpha\beta} \langle n_{\beta} \rangle. \quad (4)$$

b) *Moments.* The subleading high frequency behavior of the self energy can be used to determine some additional coefficients. In the case of the three pole approximation, we determine coefficients A_{α} , B_{α} and C_{α} from the first three moments of the self-energy $\Sigma_{\alpha}^{(1)}$, $\Sigma_{\alpha}^{(2)}$, $\Sigma_{\alpha}^{(3)}$ as follows

$$A_{\alpha} = \Sigma_{\alpha}^{(1)}, \quad (5)$$

$$B_{\alpha} = \frac{\Sigma_{\alpha}^{(2)}}{\Sigma_{\alpha}^{(1)}}, \quad (6)$$

$$C_{\alpha} = \frac{\Sigma_{\alpha}^{(3)} \Sigma_{\alpha}^{(1)} - (\Sigma_{\alpha}^{(2)})^2}{(\Sigma_{\alpha}^{(1)})^2}, \quad (7)$$

while in the two pole approximation only coefficient A_{α} should be determined from the high frequency moment, as stated in Eq. (5) above. The self-energy moments can be expressed by the occupancies and correlation functions that can be calculated within an approximation like slave-boson Gutzwiller or Hubbard I. The expressions for the self-energy moments are worked out explicitly in the Appendix A.

c) *Mass Renormalization.* If independent determination of the quasiparticle residue, Z_α , exists, the following relationship holds

$$\frac{\partial \Sigma_\alpha}{\partial i\omega} |_{i\omega=0} = 1 - Z_\alpha^{-1}. \quad (8)$$

d) *Number of particles.* Sum over all Matsubara frequencies of the Green's function gives number of particles, i.e.

$$n_\alpha = T \sum_{i\omega} G_{f\alpha}(i\omega) e^{i\omega 0^+}, \quad (9)$$

where

$$G_{f\alpha}(i\omega) = \frac{1}{i\omega - \epsilon_{f\alpha} - \Delta_\alpha(i\omega) - \Sigma_\alpha(i\omega)} \quad (10)$$

defines the impurity Green function and $\Delta_\alpha(i\omega_n)$ is the hybridization function.

e) *Friedel sum rule.*

This is a relation between the total density and the real part of the self-energy at zero frequency. It determines zero-frequency value of the self-energy

$$\begin{aligned} n_\alpha &= \frac{1}{2} + \frac{1}{\pi} \operatorname{arctg} \left(\frac{\epsilon_{f\alpha} + \Re \Sigma_\alpha(i0^+) + \Re \Delta_\alpha(i0^+)}{\Im \Delta_\alpha(i0^+)} \right) \\ &+ \int_{-i\infty}^{+i\infty} \frac{dz}{2\pi i} G_{f\alpha}(z) \frac{\partial \Delta_\alpha(z)}{\partial z} e^{z0^+}. \end{aligned} \quad (11)$$

Formally, some of the constraints [(c) and (e)] hold for zero temperature only but we expect no significant deviations as long as we stay at low temperatures.

We thus see that the interpolational scheme is defined completely once a prescription for obtaining parameters such as Z_α , n_α and $\Sigma_\alpha^{(n)}$ is given. For this purpose we will test two popular methods: slave-boson Gutzwiller method²⁰ as described by Kotliar and Ruckenstein²¹ and the well-known Hubbard I approximation²⁴. We compare these results against more accurate but computationally demanding Quantum Monte Carlo¹ calculations.

Notice that once the parameters such as Z_α are computed from a given approximate method, some of the quantities such as the total number of particles, n_α , and the value of the self-energy at zero frequency, $\Sigma_\alpha(i0)$, can be computed fully self-consistently. They can be compared with their non-self-consistent values. If the approximate scheme already provides a good approximation for n_α and satisfies the Friedel sum rule, the self-consistency can be avoided hence accelerating the calculation. Indeed we found that inclusion of the self-consistency improves the Gutzwiller results in the vicinity of the Mott transition only where the Hubbard bands get increasingly important.

We now give the description of our approximate algorithms and then present the comparison with the QMC calculations.

III. METHODS FOR SOLVING IMPURITY MODEL

A. Quantum Monte Carlo Method

The Quantum Monte Carlo method is a powerful and manifestly not perturbative approach in either interaction U or the bandwidth W . In the QMC method one introduces a Hubbard-Stratonovich field and averages over it using the Monte Carlo sampling. This is a controlled approximation using different expansion parameter, the size of the mesh for the imaginary time discretization. Unfortunately it is computationally very expensive as the number of time slices and the number of Hubbard-Stratonovich fields increases. Extensive description of this method can be found in Ref. 1. We will use this method to benchmark our calculations with approximate but much faster algorithms described below.

B. Slave-Boson Approach

A fast approach to solve a general impurity problem is the slave-boson method^{21,22,23}. At the mean field level, it gives the results similar to the famous Gutzwiller approximation²⁰. However, it is improvable by performing fluctuations around the saddle point. This approach is accurate as it has been shown recently to give the exact critical value of U in the large degeneracy limit at half-filling²⁵.

The main idea is to rewrite atomic states consisting of n electrons $|\gamma_1, \dots, \gamma_n\rangle$, $0 \leq n \leq N$ with help of a set of slave-bosons $\{\psi_n^{\gamma_1, \dots, \gamma_n}\}$. In the following, we assume $SU(N)$ symmetric case, i.e., equivalence between different states $|\gamma_1, \dots, \gamma_n\rangle$ for fixed n . Formulae corresponding to a more general crystal-field case are given in Appendix B. The creation operator of a physical electron is expressed via slave particles in the standard manner²². In order to recover the correct non-interacting limit at the mean-field level, the Bose fields ψ_n can be considered as classical values found from minimizing a Lagrangian $L\{\psi_n\}$ corresponding to the Hamiltonian (1). Two Lagrange multipliers λ and Λ should be introduced in this way, which correspond to the following two constraints:

$$\sum_{n=0}^N C_n^N \psi_n^2 = 1, \quad (12)$$

$$\sum_{n=0}^N n C_n^N \psi_n^2 = TN \sum_{i\omega} G_g(i\omega) e^{i\omega 0^+} = \bar{n}. \quad (13)$$

The physical meaning of the first constrain is that the sum of probabilities to find atom in any state is equal to one, and the second constrain gives the mean number of electrons coinciding with that found from $G_g(i\omega) = (i\omega - \lambda - b^2 \Delta(i\omega))^{-1}$. A combinatorial factor $C_n^N = \frac{N!}{n!(N-n)!}$ arrives due to assumed equivalence of all states with n electrons.

Minimization of $L\{\psi_n\}$ with respect to ψ_n leads us to the following set of equations to determine the quantities ψ_n :

$$\begin{aligned} [E_n + \Lambda - n\lambda]\psi_n + nbT \sum_{i\omega} \Delta(i\omega)G_g(i\omega)[LR\psi_{n-1} + \psi_n bL^2] + \\ + (N - n)bT \sum_{i\omega} \Delta(i\omega)G_g(i\omega)[R^2b\psi_n + LR\psi_{n+1}] = 0, \end{aligned} \quad (14)$$

where $b = RL \sum_{n=1}^N C_{n-1}^{N-1} \psi_n \psi_{n-1}$, determines the mass renormalization, and the coefficients $L = (1 - \sum_{n=1}^N C_{n-1}^{N-1} \psi_n^2)^{-1/2}$, $R = (1 - \sum_{n=0}^N C_n^{N-1} \psi_n^2)^{-1/2}$ are normalization constants as in Refs. 21,22. $E_n = \epsilon_f n + Un(n-1)/2$ is the total energy of the atom with n electrons within $SU(N)$ approximation.

Eq. (14), along with the constraints (12), (13) constitute a set of non-linear equations which have to be solved iteratively. In practice, we consider Eq. (14) as an eigenvalue problem with Λ being the eigenvalue and ψ_n being the eigenvectors of the matrix. The physical root corresponds to the lowest eigenvalue of Λ which gives a set of ψ_n determining the mass renormalization $Z = b^2$. Since the matrix to be diagonalized depends non-linearly on ψ_n via the parameters L , R , and b and also on λ , the solution of the whole problem assumes the self-consistency: (i) we build an initial approximation to ψ_n (for example the Hartree-Fock solution) and fix some λ , (ii) we solve eigenvalue problem and find new normalized ψ_n , (iii) we mix new ψ_n with the old ones using the Broyden method²⁶ and build new L , R , and b . Steps (ii) and (iii) are repeated until the self-consistency with respect to ψ_n is reached. During the iterations we also vary λ to obey the constraints. The described procedure provides a stable computational algorithm for solving AIM and gives us an access to the low-frequency Green's function and the self-energy of the problem via knowledge of the slope of $\Im\Sigma(i\omega)$ and the value $\Re\Sigma(0)$ at zero frequency.

The described slave-boson method gives the following expression for the self-energy:

$$\Sigma(i\omega) = (1 - b^{-2})i\omega - \epsilon_f + \lambda b^{-2}. \quad (15)$$

The impurity Green function $G_f(i\omega)$ in this limit is given by the expression

$$G_f(i\omega) = b^2 G_g(i\omega). \quad (16)$$

As an illustration, we now give the solution of Eq. (14) for non-degenerate case ($N = 2$) and at the particle-hole symmetry point with $\epsilon_{imp} - \mu = -\frac{U}{2}(N - 1)$. Consider a dynamical mean-field theory for the Hubbard model which reduces the problem to solving the impurity model subject to the self-consistency condition with respect to $\Delta(i\omega)$. Starting with the semicircular density of states (DOS), the self-consistency condition is given by $\Delta(i\omega) = t^2 G_f(i\omega)$ with parameter t being the quarter of bandwidth. We obtain the following simplifications:

$L = R = \sqrt{2}$, $\lambda = 0$, $\psi_0 = \psi_2$, $b = 4\psi_1\psi_2$ and $G_g(i\omega) = [i\omega - t^2 b^2 G_g(i\omega)]^{-1}$. The sum $T \sum_{i\omega} \Delta(i\omega)G_g(i\omega)$ appeared in Eq. (14) scales as $2ta$ with the constant α being the characteristic of a particular density of states and approximately equal to -0.2 in the semicircular DOS case. The self-consistent solution of Eq. (14) is therefore possible and simply gives $\psi_2^2 = \frac{U}{128ta} + \frac{1}{4}$. The Mott transition occurs when no sites with double occupancies can be found, i.e. when $\psi_0 = \psi_2 = 0$. A critical value of $U_c = 32t|\alpha| = 8W|\alpha|$ with W being the bandwidth. For $\alpha \approx -0.2$, this gives $U_c \approx 1.6W$ and reproduces the exact result for $U_c = 1.49W$ within a few percent accuracy. As degeneracy increases, critical U is shifted towards higher values. From numerical calculations we obtained the following values of the critical interactions in the half-filled case $U_c \approx 3W$ for $N = 6$ (p -level), $U_c \approx 4.5W$ for $N = 10$ (d -level), and $U_c \approx 6W$ for $N = 14$ (f -level).

Density-density correlation function $\langle n_\alpha n_\beta \rangle$ (where $\alpha \neq \beta$) for local states with n electrons is proportional to the number of pairs formed by n particles C_2^n/C_2^N . Since the probability for n electrons to be occupied is given by: $P_n = \psi_n^2 C_n^N$, the physical density-density correlator can be deduced from: $\langle nn \rangle = \sum_n C_2^n/C_2^N P_n$. Similarly, the triple occupancy can be calculated from: $\langle nnn \rangle = \sum_n C_3^n/C_3^N P_n$.

Let us now check the accuracy of this method by comparing its results with the QMC data. We consider the two-band Hubbard model within $SU(4)$ orbitally degenerate case. Hybridization $\Delta(i\omega) = \sum_{\mathbf{k}} V(\mathbf{k})/(i\omega - E_{\mathbf{k}})$ satisfies the DMFT self-consistency condition of the Hubbard model on a Bethe lattice

$$\Delta(i\omega) = t^2 G(i\omega), \quad (17)$$

where t is a quarter of the bandwidth W . The Coulomb interaction is chosen to be $U = 4d$ (d is the half-bandwidth) which is sufficiently large to open the Mott gap at integer fillings. All calculations are done for the temperature $T = 1/16d$.

We first compare the average number of electrons vs. chemical potential determined from the slave bosons which is plotted in Fig. 1(a). This quantity is sensitive to the low-frequency part of the Green function which should be described well by the present method. We see that it reproduces the QMC data with a very high accuracy. The quasiparticle residue $Z = 1/(1 - \frac{\partial \Im\Sigma(i\omega)}{\partial i\omega})|_{i\omega \rightarrow 0}$ versus filling \bar{n} is plotted in Fig. 1(b). The slave-boson method gives the Fermi liquid and provides a good estimate for the quasiparticle residue. Indeed, the agreement with the QMC results is satisfactory. Also, recent findings²⁵ suggest that at half-filling Z deduced from slave bosons becomes exact when $N \rightarrow \infty$. Still the discrepancy of the order of 30% can be found. In fact, we have performed several additional calculations for other degeneracies ($N = 2$ and 6) and for various parameters regimes. The trend to underestimate mass renormalization by about 30% can be seen in almost all cases (it disappears only when U approaches zero). This empirical finding is useful as we can use the reduced values of

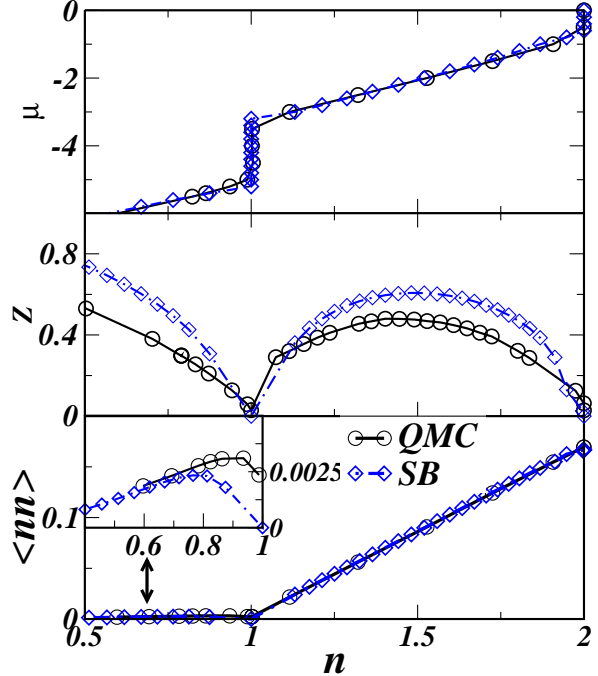


FIG. 1: Comparison between the slave boson mean field and the QMC calculation for (a) concentration versus chemical potential, (b) dependence of the spectral weight Z on concentration, and (c) density-density correlation function, $\langle n_\alpha n_{\alpha'} \rangle$ versus filling, \bar{n} , in the two-band Hubbard model.

Z needed for our interpolating formula.

Fig. 1(c) shows the density-density correlation function $\langle n_\alpha n_{\alpha'} \rangle$ as a function of average occupation \bar{n} . The discrepancy is most pronounced for fillings $\bar{n} < 1$ [see the inset of Fig. 1(c)] where the absolute values of $\langle n_\alpha n_{\alpha'} \rangle$ are rather small. Although our slave-boson technique captures only the quasiparticle peak, it gives the correlation function in reasonable agreement with the QMC for dopings not too close to the Mott transition.

C. Hubbard I Approximation

Now we turn to the Hubbard I approximation²⁴ which is closely related to the moments expansion method²⁷. One introduces Hubbard operators and the corresponding Green function $G_{nm}(i\omega)$ defined for these Hubbard operators. Within $SU(N)$ we are summing over certain set of Hubbard operators which induce transitions between n -times and $n+1$ -times occupied local level. The impurity Green function is

$$G_f(i\omega) = \sum_{nm} G_{nm}(i\omega), \quad (18)$$

where the matrix $[G_{nm}(i\omega)]^{-1} = [G_{nm}^{at}(i\omega)]^{-1} - \Delta(i\omega)$, $n, m = 0, N-1$. $G_{nm}^{at}(i\omega)$ is the atomic Green function

$$G_{nm}^{at}(i\omega) = \delta_{nm} \frac{C_n^{N-1}(X_n + X_{n+1})}{i\omega + \mu - E_{n+1} + E_n}. \quad (19)$$

The coefficients X_n are the probabilities to find atom with n electrons similar to the coefficients ψ_n^2 introduced above. They can be also used to find the averages $\langle nn \rangle$ in the same way. These numbers are normalized to unity, $\sum_{n=0}^N C_n^N X_n = \sum_{n=0}^{N-1} C_n^{N-1}(X_n + X_{n+1}) = 1$, and are expressed via diagonal elements of $G_{nm}(i\omega)$ as follows: $X_n = -T \sum_{i\omega} G_{nn}(i\omega) e^{-i\omega 0^+} / C_n^{N-1}$. The mean number of electrons can be measured as follows: $\bar{n} = \sum_{n=0}^N n C_n^N X_n$ or as: $\bar{n} = TN \sum_{i\omega} G_f(i\omega) e^{i\omega 0^+}$.

Note that when $\Delta(i\omega) \equiv 0$, $G_f(i\omega)$ is reduced to $\sum_{nm} G_{nm}^{at}(i\omega)$, i.e. Hubbard I reproduces the atomic limit. Setting $U \equiv 0$ gives $G_f(i\omega) = [i\omega + \mu - \epsilon_f - \Delta(i\omega)]^{-1}$, which is the correct band limit. Unfortunately, at half-filling this limit has a pathology connected to the instability towards Mott transition at any interaction strength U . To see this, we consider a dynamical mean-field theory for the Hubbard model. Using semicircular density of states, we obtain $G_f(i\omega) = [1 - t^2 G_f(i\omega) G_{at}(i\omega)]^{-1} G_{at}(i\omega)$ and conclude that for any small U the system opens a pathological gap in the spectrum. Clearly, using Hubbard I only, the behavior of the Green function at $i\omega \rightarrow 0$ cannot be reproduced. This emphasizes the importance of using the slave-boson treatment at small frequencies.

Let us now check the accuracy of this method against QMC. We again consider the two-band Hubbard model within $SU(4)$ symmetry as in the case of the slave-boson method described earlier. The $\bar{n}(\mu)$ is plotted in Fig. 2(a). The Hubbard I approximation does not give satisfactory agreement with the QMC data because it misses the correct behavior at low frequencies. The comparisons for $Z(\bar{n})$ is plotted in Fig. 2(b). These numbers are extracted from the low-frequency slope of the imaginary part of the self-energy on the imaginary axis. Surprisingly, the Hubbard I Z 's show a relatively good behavior when comparing to the QMC method. However, the pathology of this approximation at half-filling would predict $Z = 0$ for any U , which is a serious warning not to use it for extracting the quasiparticle weight. Fig. 2(c) shows $\langle nn \rangle$ as a function of average occupation \bar{n} . As this quantity is directly related to the high-frequency expansion one may expect a better accuracy here. However, comparing Fig. 2(c) and Fig. 1(c), it is clear that the slave boson method gives more accurate double occupancy. This is due to the fact that the density matrix obtained by the slave boson method is of higher quality than the one obtained from the Hubbard I approximation.

The results of these calculations suggest that the slave-boson Gutzwiller method shows a good accuracy in comparison with the QMC. Therefore it can be used to determine the unknown coefficients in the interpolational form of the self-energy, Eqs. (2) or (3). At the same time the use of the Hubbard approximation should be avoided. Interestingly, while more sophisticated QMC approach captures both the quasiparticle peak and the Hubbard bands this is not the case for the slave-boson mean field method. To obtain the Hubbard bands in this

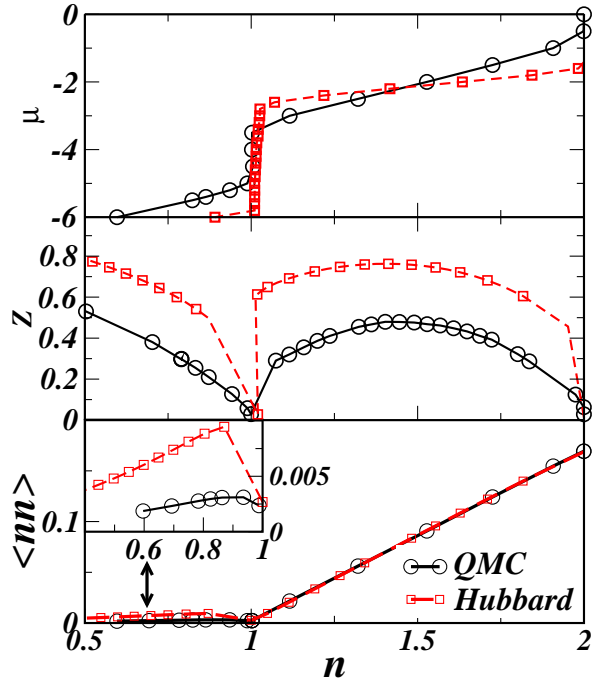


FIG. 2: Comparison between the Hubbard I and the QMC calculation for (a) concentration versus chemical potential, (b) dependence of the spectral weight Z on concentration, and (c) density-density correlation function, $\langle n_\alpha n_{\alpha'} \rangle$ versus filling, \bar{n} , in the two-band Hubbard model.

method fluctuations need to be computed, which would be very tedious in a general multiorbital situation. However the slave–boson method delivers many parameters in a good agreement with the QMC results, and hence it can be used to obtain the parameters that enter the rational approximation. In this way slave–boson approach generates a better Green function with quasiparticles and Hubbard bands *at no extra computational cost*.

IV. RESULTS OF THE INTERPOLATIVE SCHEME

We now turn to the comparison of the self-energy obtained using the formula (3) and the corresponding Green functions after the formula (10) against the predictions of the Quantum Monte Carlo method. We have studied the results of the two-pole and the three-pole interpolations which require the determination of either 4 or 6 coefficients. The interpolational formula with two-poles needs finding the values of $\Sigma(0)$, Z and the first high-frequency moment of the self-energy $\Sigma^{(1)}$. The condition that the total number of electrons found from the Green function (10) is the same as predicted by the slave–boson method can be used to fix the fourth coefficient. To explore the three-pole interpolation, two more conditions are required. We have used additional high frequency moments $\Sigma^{(2)}$, and $\Sigma^{(3)}$ which can be determined if one computes correlational functions $\langle nn \rangle$, $\langle nnn \rangle$, $\langle nnnn \rangle$.

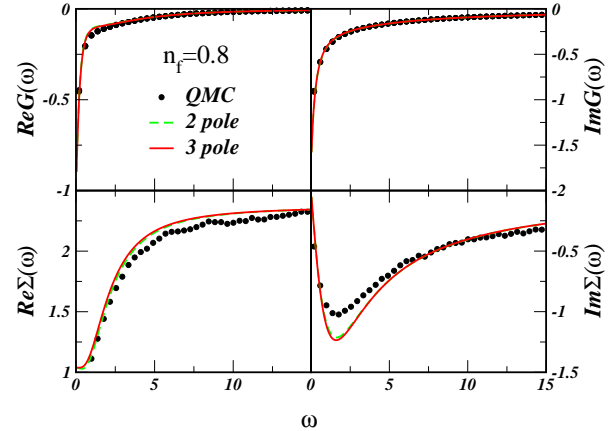


FIG. 3: Comparison between real and imaginary parts of the Green function and the self-energy obtained from the interpolative method and the Quantum Monte Carlo calculation for the two-band Hubbard model at filling $\bar{n} = 0.8$.

We perform the comparison of the interpolational scheme against QMC for two characteristic values of the concentrations: $\bar{n} = 0.8$ representing the case $\bar{n} < 1$ and $\bar{n} = 1.2$ representing the case $\bar{n} > 1$. Both cases are chosen to be close to the Mott transition. This is a hard test for our approach as we have found that the predictions of the interpolational scheme and the QMC data are practically indistinguishable in the metallic region far from the Mott transition ($U \lesssim W$). The two-band

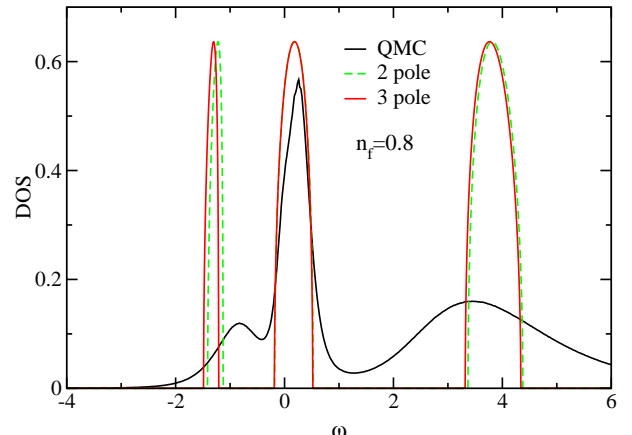


FIG. 4: Comparison between the one-electron densities of states obtained from interpolative formula and the Quantum Monte Carlo calculation for the two-band Hubbard model at filling $\bar{n} = 0.8$.

Fig. 3 shows the comparison of the real and imaginary parts of the self-energy and the Green function obtained by the two- and three-pole interpolations with the QMC results. Both interpolational schemes give pretty good

agreement at all frequencies. These results are obtained with the values of mass renormalizations Z reduced by 30% which gives a better agreement with Z_{QMC} as we discussed in Section III. The results with bare Z 's deduced from the slave-boson method are also found to be quite accurate but not as good as we advertise in Fig. 3. We have also performed the comparison for the one-electron density of states which are shown in Fig. 4. One can see the appearance of the lower and upper Hubbard bands as well as renormalized quasiparticle peak.

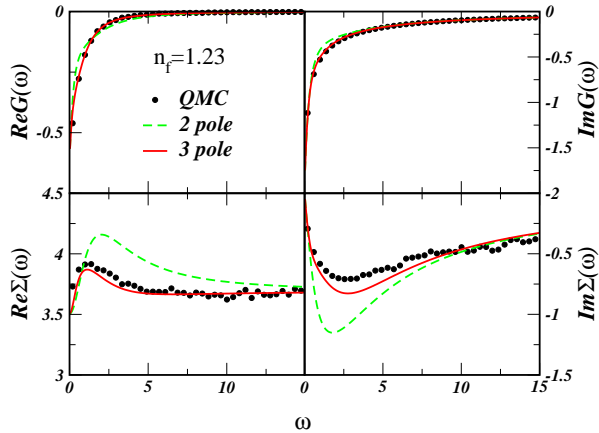


FIG. 5: Comparison between real and imaginary parts of the Green function and the self-energy obtained from the interpolative method and the Quantum Monte Carlo calculation for the two-band Hubbard model at filling $\bar{n} = 1.23$.

In Fig. 5, we show our results for the case $\bar{n} = 1.2$ using the two- and three-pole interpolational formula (3). As far as the two-pole scheme is concerned, the overall agreement is satisfactory but a discrepancy exists in the region of intermediate imaginary frequencies. It is directly related to the misplaced upper Hubbard band as can be seen in Fig. 6. This discrepancy disappears in the three-pole interpolation as is evident from the Fig. 5. Comparison of the one-electron density of states is shown in Fig. 6. Clearly, the two-pole interpolation is inadequate in this regime, while the three-pole interpolating scheme gives correct position of Hubbard bands and quasiparticle peak, all basic features of the Anderson impurity problem.

Finally, we would like to comment on the renormalization of the quasiparticle residue Z beyond the slave boson mean-field result. While we found empirically that the 30% renormalization significantly improves our fits to the QMC data, over a broad region of parameters, this cannot hold everywhere since Z should go to 1 when U approaches zero. The reduction of Z beyond the mean-field results, in the regions where the correlations are strong, can be thought to arise from fluctuation corrections of

the slave boson around the saddle point value. A computationally efficient way to evaluate these corrections, which will also give rise to the quasiparticle lifetime not included in this paper, are important open problems left

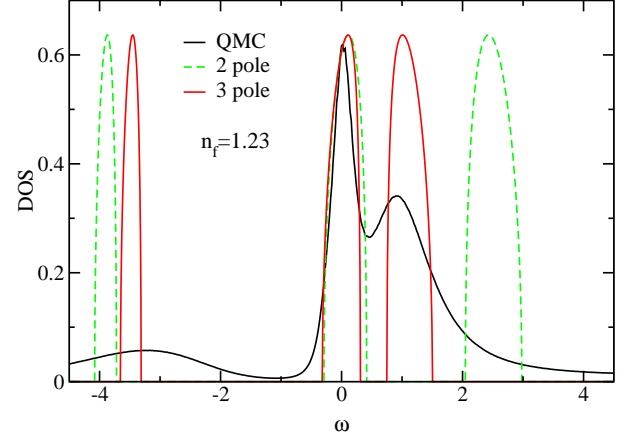


FIG. 6: Comparison between the one-electron densities of states obtained from interpolative formula and the Quantum Monte Carlo calculation for the two-band Hubbard model at filling $\bar{n} = 1.23$.

V. CONCLUSION

To summarize, this paper shows the possibility to extract parameters for the interpolating self-energy of the Anderson impurity model such as the self-energy at zero frequency, the mass renormalization, the density and the high frequency moments using computationally very efficient slave-boson mean field approach. These data are then used to reconstruct the self-energy at all frequencies using a rational interpolation formula. We find that three-pole interpolation predicts the self-energy quite accurately as compared to the results of more sophisticated approaches such as the Quantum Monte Carlo method.

As a general conclusion, we have thus found that interpolative formulae with several poles are sufficient to fit the self-energies in a broad range of the parameters of the quantum impurity problem and the slave-boson mean-field method is capable to deliver all necessary ingredients for this algorithm. The approach can be used for the evaluation of LDA+DMFT total energies and is a very direct way to obtain spectra with a three-peak structure, characteristic of the strongly correlated regime, with very little computational effort.

The work was supported by NSF-DMR Grants 0096462, 02382188, 0312478, 0342290 and US DOE Grant No DE-FG02-99ER45761. The authors also acknowledge the financial support from the Computational Material Science Network operated by US DOE and from the Ministry of Education, Science and Sport of Slovenia.

VI. APPENDIX A

High-frequency moment expansions for the Green function and the self-energy can be worked out:

$$G_\alpha(i\omega) = \frac{G_\alpha^{(1)}}{\omega} + \frac{G_\alpha^{(2)}}{\omega^2} + \frac{G_\alpha^{(3)}}{\omega^3} \dots, \quad (20)$$

where the moments of the Green function are given by the following formulae

$$G_\alpha^{(1)} = 1, \quad (21)$$

$$G_\alpha^{(2)} = \epsilon_{f\alpha} + \sum_\beta U_{\alpha\beta} \langle n_\beta \rangle, \quad (22)$$

$$G_\alpha^{(3)} = \epsilon_{f\alpha}^2 + 2\epsilon_{f\alpha} \sum_\beta U_{\alpha\beta} \langle n_\beta \rangle + \sum_{\beta\beta'} U_{\alpha\beta} U_{\alpha\beta'} \langle n_\beta n_{\beta'} \rangle + \sum_{\mathbf{k}} |V_\alpha(\mathbf{k})|^2, \quad (23)$$

$$\begin{aligned} G_\alpha^{(4)} = & \epsilon_{f\alpha}^3 + 3\epsilon_{f\alpha}^2 \sum_\beta U_{\alpha\beta} \langle n_\beta \rangle + 3\epsilon_{f\alpha} \sum_{\beta\beta'} U_{\alpha\beta} U_{\alpha\beta'} \langle n_\beta n_{\beta'} \rangle + \sum_{\beta\beta'\beta''} U_{\alpha\beta} U_{\alpha\beta'} U_{\alpha\beta''} \langle n_\beta n_{\beta'} n_{\beta''} \rangle, \\ & + \sum_{\mathbf{k}} |V_\alpha(\mathbf{k})|^2 (E_{\mathbf{k}\alpha} + 2\epsilon_{f\alpha} + 2 \sum_\beta U_{\alpha\beta} \langle n_\beta \rangle) + \sum_{\mathbf{k},\beta} U_{\alpha\beta}^2 V_\beta(\mathbf{k}) \langle (2n_\alpha - 1) f_\beta^\dagger c_{\mathbf{k}\beta} \rangle. \end{aligned} \quad (24)$$

The expansion for the self-energy is obtained as follows

$$\Sigma_\alpha(i\omega) = \omega + \mu - \Delta_\alpha(i\omega) - \left(\frac{G_\alpha^{(1)}}{\omega} + \frac{G_\alpha^{(2)}}{\omega^2} + \frac{G_\alpha^{(3)}}{\omega^3} + \dots \right)^{-1} = \Sigma_\alpha(i\infty) + \frac{\Sigma_\alpha^{(1)}}{\omega} + \frac{\Sigma_\alpha^{(2)}}{\omega^2} + \frac{\Sigma_\alpha^{(3)}}{\omega^3} \dots, \quad (25)$$

where the self-energy moments are given by

$$\Sigma_\alpha^{(1)} = G_\alpha^{(3)} - [G_\alpha^{(2)}]^2 - \sum_k |V_k|^2 = \sum_{\beta\beta'} U_{\alpha\beta} U_{\alpha\beta'} (\langle n_\beta n_{\beta'} \rangle - \langle n_\beta \rangle \langle n_{\beta'} \rangle), \quad (26)$$

$$\begin{aligned} \Sigma_\alpha^{(2)} = & G_\alpha^{(4)} - 2G_\alpha^{(2)} G_\alpha^{(3)} + [G_\alpha^{(2)}]^3 - \sum_{\mathbf{k}} |V_\alpha(\mathbf{k})|^2 E_{\mathbf{k}\alpha} = \\ = & \sum_{\beta\beta'\beta''} U_{\alpha\beta} U_{\alpha\beta'} U_{\alpha\beta''} (\langle n_\beta n_{\beta'} n_{\beta''} \rangle - 2\langle n_\beta n_{\beta'} \rangle \langle n_{\beta''} \rangle + \langle n_\beta \rangle \langle n_{\beta'} \rangle \langle n_{\beta''} \rangle) \\ & + \epsilon_{f\alpha} \sum_{\beta\beta'} U_{\alpha\beta} U_{\alpha\beta'} (\langle n_\beta n_{\beta'} \rangle - \langle n_\beta \rangle \langle n_{\beta'} \rangle) + \sum_{\mathbf{k},\beta} U_{\alpha\beta}^2 V_\beta(\mathbf{k}) \langle (2n_\alpha - 1) d_\beta^\dagger c_{\mathbf{k}\beta} \rangle, \end{aligned} \quad (27)$$

$$\begin{aligned} \Sigma_\alpha^{(3)} = & G_\alpha^{(5)} - 2G_\alpha^{(4)} G_\alpha^{(2)} - \left[G_\alpha^{(3)} \right]^2 + 3G_\alpha^{(3)} \left[G_\alpha^{(2)} \right]^2 - \left[G_\alpha^{(2)} \right]^4 - \sum_{\mathbf{k}} |V_\alpha(\mathbf{k})|^2 E_{\mathbf{k}\alpha}^2 = \\ = & \sum_{\beta_1\beta_2\beta_3\beta_4} U_{\alpha\beta_1} U_{\alpha\beta_2} U_{\alpha\beta_3} U_{\alpha\beta_4} (\langle n_{\beta_1} n_{\beta_2} n_{\beta_3} n_{\beta_4} \rangle - 2\langle n_{\beta_1} n_{\beta_2} n_{\beta_3} \rangle \langle n_{\beta_4} \rangle - \langle n_{\beta_1} n_{\beta_2} \rangle \langle n_{\beta_3} n_{\beta_4} \rangle \\ & + 3\langle n_{\beta_1} n_{\beta_2} \rangle \langle n_{\beta_3} \rangle \langle n_{\beta_4} \rangle - \langle n_{\beta_1} \rangle \langle n_{\beta_2} \rangle \langle n_{\beta_3} \rangle \langle n_{\beta_4} \rangle) \\ & + 2\epsilon_\alpha \sum_{\beta_1\beta_2\beta_3} U_{\alpha\beta_1} U_{\alpha\beta_2} U_{\alpha\beta_3} (\langle n_{\beta_1} n_{\beta_2} n_{\beta_3} \rangle - 2\langle n_{\beta_1} n_{\beta_2} \rangle \langle n_{\beta_3} \rangle + \langle n_{\beta_1} \rangle \langle n_{\beta_2} \rangle \langle n_{\beta_3} \rangle) \\ & + \epsilon_\alpha^2 \sum_{\beta_1\beta_2} U_{\alpha\beta_1} U_{\alpha\beta_2} (\langle n_{\beta_1} n_{\beta_2} \rangle - \langle n_{\beta_1} \rangle \langle n_{\beta_2} \rangle) + \mathcal{N}_\alpha^{(3)}. \end{aligned} \quad (28)$$

The nonlocal part of the self-energy moment, which explicitly depends on hybridization matrix V and vanishes in the atomic limit, is explicitly quoted only for the second moment (last term in Eq. (27)). In the third order, the nonlocal term is denoted by $\mathcal{N}_\alpha^{(3)}$ and has not yet been evaluated. In practical calculations, we neglected it's contribution.

Within $SU(N)$ symmetric case the formulae are simplified. First, introduce the definitions:

$$\langle n \rangle = \sum_{n=1}^N \frac{n}{N} C_n^N \psi_n^2 \quad (29)$$

$$\langle nn \rangle = \sum_{n=1}^N \frac{C_2^n}{C_2^N} C_n^N \psi_n^2 \quad (30)$$

$$\langle nnn \rangle = \sum_{n=1}^N \frac{C_3^n}{C_3^N} C_n^N \psi_n^2 \quad (31)$$

$$\kappa = \frac{LR}{Z} \sum_{n=1}^N C_{n-2}^{N-2} \psi_{n-1} \psi_n \quad (32)$$

where ψ_n^2 is probability for n times occupancy (with n electrons on the local level). Then

$$\sum_{\beta} U_{\alpha\beta} \langle n_{\beta} \rangle = U(N-1) \langle n \rangle, \quad (33)$$

$$\sum_{\beta\beta'} U_{\alpha\beta} U_{\alpha\beta'} \langle n_{\beta} n_{\beta'} \rangle = U^2 [(N-1)(N-2) \langle nn \rangle + (N-1) \langle n \rangle], \quad (34)$$

$$\sum_{\beta\beta'\beta''} U_{\alpha\beta} U_{\alpha\beta'} U_{\alpha\beta''} \langle n_{\beta} n_{\beta'} n_{\beta''} \rangle = U^3 [(N-1)(N-2)(N-3) \langle nnn \rangle + 3(N-1)(N-2) \langle nn \rangle + (N-1) \langle n \rangle], \quad (35)$$

$$\sum_{\mathbf{k}\beta} U_{\alpha\beta}^2 V_{\beta}(\mathbf{k}) \langle (2n_{\alpha} - 1) f_{\beta}^{\dagger} c_{\mathbf{k}\beta} \rangle = (N-1)(ZU)^2 (1-2\kappa) \int \frac{d\xi}{\pi} f(\xi) \text{Im}\{\Delta(\xi) G_g(\xi)\}. \quad (36)$$

Introducing the notations

$$\int \frac{d\xi}{\pi} f(\xi) \text{Im}\{\Delta(\xi) G_g(\xi)\} = \Delta G_g \quad (37)$$

we, for example, obtain the following formulae

$$\Sigma^{(1)} = [(N-1)(N-2) \langle nn \rangle + (N-1) \langle n \rangle - (N-1)^2 \langle n \rangle^2] U^2, \quad (38)$$

$$\begin{aligned} \Sigma^{(2)} &= (N-1)(N-2)(N-3) \langle nnn \rangle U^3 + (N-1)(N-2) \langle nn \rangle (3U^3 + \epsilon_f U^2 - 2(N-1) \langle n \rangle U^3), \\ &+ (N-1)^3 \langle n \rangle^3 U^3 - (N-1)^2 \langle n \rangle^2 (2U^3 + \epsilon_f U^2) + (N-1) \langle n \rangle (U^3 + \epsilon_f U^2) + (N-1)(ZU)^2 (1-2\kappa) \Delta G_g \end{aligned} \quad (39)$$

VII. APPENDIX B

In the crystal field case we assume that N -fold degenerate impurity level ϵ_f is split by a crystal field onto G sublevels $\epsilon_{f1}, \dots, \epsilon_{f\alpha}, \dots, \epsilon_{fG}$. We assume that for each sublevel there is still some partial degeneracy d_{α} so that $\sum_{\alpha=1}^G d_{\alpha} = N$. In limiting case of $SU(N)$ degeneracy, $G = 1, d_1 = N$, and in non-degenerate case, $G = N, d_1 = d_{\alpha} = d_G = 1$. We need to discuss how a number of electrons n can be accommodated over different sublevels $\epsilon_{f\alpha}$. Introducing numbers of electrons on each sublevel, n_{α} , we obtain $\sum_{\alpha=1}^G n_{\alpha} = n$. Note the restrictions: $0 < n < N$, and $0 < n_{\alpha} \leq d_{\alpha}$. In $SU(N)$ case, $G = 1, n_1 = n$, and in non-degenerate case, $G = N, n_{\alpha}$ is either 0 or 1. Total energy for the shell with n electrons depends on particular configuration $\{n_{\alpha}\}$

$$E_{n_1 \dots n_G} = \sum_{\alpha=1}^G \epsilon_{f\alpha} n_{\alpha} + \frac{1}{2} U (\Sigma_{\alpha} n_{\alpha}) [(\Sigma_{\alpha} n_{\alpha}) - 1]. \quad (40)$$

Many-body wave function is also characterized by a set of numbers $\{n_{\alpha}\}$, i.e. $|n_1 \dots n_G\rangle$. Energy $E_{n_1 \dots n_G}$ remains degenerate, which can be calculated as product of how many combinations exists to accommodate electrons in each sublevel, i.e. $C_{n_1}^{d_1} \times \dots \times C_{n_{\alpha}}^{d_{\alpha}} \times \dots \times C_{n_G}^{d_G}$. Let us further introduce probabilities $\psi_{n_1 \dots n_G}$ to find a shell in a given state with energy $E_{n_1 \dots n_G}$. Sum of all probabilities should be equal to 1, i.e.

$$\sum_{n_1=0}^{d_1} \dots \sum_{n_{\alpha}=0}^{d_{\alpha}} \dots \sum_{n_G=0}^{d_G} C_{n_1}^{d_1} \dots C_{n_{\alpha}}^{d_{\alpha}} \dots C_{n_G}^{d_G} \psi_{n_1 \dots n_G}^2 = 1. \quad (41)$$

There are two Green functions in Gutzwiller method: impurity Green function $\hat{G}_f(i\omega)$ and quasiparticle Green function $\hat{G}_g(i\omega) = \hat{b}^{-1}\hat{G}_f(i\omega)\hat{b}^{-1}$, where matrix coefficients \hat{b} represent generalized mass renormalizations parameters. All matrices assumed to be diagonal and having diagonal elements numerated as follows: $G_1(i\omega), \dots G_\alpha(i\omega), \dots G_G(i\omega)$. Each element in the Green function is represented as follows

$$G_{g\alpha}(i\omega) = \frac{1}{i\omega - \lambda_\alpha - b_\alpha^2 \Delta_\alpha(i\omega)}, \quad (42)$$

$$G_{f\alpha}(i\omega) = b_\alpha^2 G_{g\alpha}(i\omega). \quad (43)$$

and determines a mean number of electrons in each sublevel

$$\bar{n}_\alpha = d_\alpha T \sum_{i\omega} G_{g\alpha}(i\omega) e^{i\omega 0^+}. \quad (44)$$

The total mean number of electrons is thus: $\bar{n} = \sum_{\alpha=1}^G \bar{n}_\alpha$. Hybridization function $\hat{\Delta}(i\omega)$ is the matrix assumed to be diagonal and having diagonal elements numerated as follows: $\Delta_1(i\omega), \dots \Delta_\alpha(i\omega), \dots \Delta_G(i\omega)$. Mass renormalizations $Z_\alpha = b_\alpha^2$ are determined in each sublevel.

Diagonal elements for the self-energy are

$$\Sigma_\alpha(i\omega) = i\omega - \epsilon_{f\alpha} - \Delta_\alpha(i\omega) - G_\alpha^{-1}(i\omega) = i\omega \left(1 - \frac{1}{b_\alpha^2}\right) - \epsilon_{f\alpha} - \frac{\lambda_\alpha}{b_\alpha^2}. \quad (45)$$

Here:

$$b_\alpha = R_\alpha L_\alpha \sum_{n_1=0}^{d_1} \dots \sum_{n_\alpha=1}^{d_\alpha} \dots \sum_{n_G=0}^{d_G} C_{n_1}^{d_1} \dots C_{n_\alpha-1}^{d_\alpha-1} \dots C_{n_G}^{d_G} \psi_{n_1 \dots n_\alpha \dots n_G} \psi_{n_1 \dots n_\alpha-1 \dots n_G}, \quad (46)$$

$$L_\alpha = \left(1 - \sum_{n_1=0}^{d_1} \dots \sum_{n_\alpha=1}^{d_\alpha} \dots \sum_{n_G=0}^{d_G} C_{n_1}^{d_1} \dots C_{n_\alpha-1}^{d_\alpha-1} \dots C_{n_G}^{d_G} \psi_{n_1 \dots n_\alpha \dots n_G}^2 \right)^{-1/2}, \quad (47)$$

$$R_\alpha = \left(1 - \sum_{n_1=0}^{d_1} \dots \sum_{n_\alpha=0}^{d_\alpha-1} \dots \sum_{n_G=0}^{d_G} C_{n_1}^{d_1} \dots C_{n_\alpha}^{d_\alpha-1} \dots C_{n_G}^{d_G} \psi_{n_1 \dots n_\alpha \dots n_G}^2 \right)^{-1/2}. \quad (48)$$

The generalization of the non-linear equations (14) has the form

$$\begin{aligned} 0 = & [E_{n_1 \dots n_G} + \Lambda - (\Sigma_\alpha^G \lambda_\alpha n_\alpha)] \psi_{n_1 \dots n_G} + \\ & \sum_{\alpha=1}^G n_\alpha [T \Sigma_{i\omega} \Delta_\alpha(i\omega) G_{g\alpha}(i\omega)] b_\alpha [R_\alpha L_\alpha \psi_{n_1 \dots n_\alpha-1 \dots n_G} + b_\alpha L_\alpha^2 \psi_{n_1 \dots n_\alpha \dots n_G}] + \\ & \sum_{\alpha=1}^G (d_\alpha - n_\alpha) [T \Sigma_{i\omega} \Delta_\alpha(i\omega) G_{g\alpha}(i\omega)] b_\alpha [R_\alpha L_\alpha \psi_{n_1 \dots n_\alpha+1 \dots n_G} + b_\alpha R_\alpha^2 \psi_{n_1 \dots n_\alpha \dots n_G}]. \end{aligned} \quad (49)$$

¹ For a review, see, A. Georges, G. Kotliar, W. Krauth, and M. Rozenberg, Rev. Mod. Phys. **68**, 13 (1996).

² For a review, see, e.g., *Theory of the Inhomogeneous Electron Gas*, edited by S. Lundqvist and S. H. March (Plenum, New York, 1983).

³ V. I. Anisimov, A. I. Poteryaev, M. A. Korotin, A. O. Anokhin, and G. Kotliar, J. Phys.: Condens. Matter **35**, 7359 (1997).

⁴ A. Lichtenstein and M. Katsnelson, Phys. Rev. B **57**, 6884 (1998).

⁵ S. Biermann, F. Aryasetiawan, A. Georges, Phys. Rev. Lett. **90**, 086402 (2003).

⁶ I.A. Nekrasov, K. Held, N. Blumer, A.I. Poteryaev, V.I. Anisimov, and D. Vollhardt, Eur. Phys. J. B **18**, 55 (2000).

⁷ K. Held, G. Keller, V. Eyert, D. Vollhardt, V.I. Anisimov, Phys. Rev. Lett. **86**, 5345 (2001).

⁸ A. I. Lichtenstein, M. I. Katsnelson, G. Kotliar, Phys. Rev. Lett. **87**, 067205 (2001).

⁹ K. Held, A.K. McMahan, R.T. Scalettar, Phys. Rev. Lett. **87**, 276404 (2001).

¹⁰ S. Savrasov, G. Kotliar, and E. Abrahams, Nature **410**, 793 (2001).

¹¹ Xi Dai, S. Savrasov, G. Kotliar, A. Migliori, H. Ledbetter and E. Abrahams, Science **300**, 953 (2003).

¹² K. Held *et al.*, Psi-k Newsletter #56 (April 2003), p. 65; A. I. Lichtenstein, M. I. Katsnelson, and G. Kotliar, in *Electron Correlations and Materials Properties*, ed. by A. Gonis, N. Kioussis and M. Ciftan (Kluwer Academic, Plenum Publishers, 2002) p. 428.

¹³ P. W. Anderson, Phys. Rev. **124**, 41 (1961).

¹⁴ For a review, see, e.g., M. Jarrell, and J. E. Gubernatis, Physics Reports, **269**, 133 (1996).

¹⁵ H. Jeschke and G. Kotliar, Rutgers University preprint.

¹⁶ S. Florens and A. Georges Phys. Rev. B **66**, 165111 (2002).

¹⁷ K. Haule, S. Kirchner, J. Kroha, and P. Wölfle, Phys. Rev. B **64**, 155111 (2001).

¹⁸ S. H. Vosko, L. Wilk, and M. Nusair, Can. J. Phys. **58**, 1200 (1980).

¹⁹ D. M. Ceperley and B. J. Alder, Phys. Rev. Lett. **45**, 566 (1980).

²⁰ M. Gutzwiller, Phys. Rev. **134**, A923 (1964).

²¹ G. Kotliar and A. E. Ruckenstein, Phys. Rev. Lett. **57**, 1362 (1986).

²² R. Fresard and G. Kotliar, Phys. Rev. B. **56**, 12909 (1997).

²³ H. Hasegawa, Phys. Rev. B **56**, 1196 (1997).

²⁴ J. Hubbard, Proc. Roy. Soc. (London) A**281**, 401 (1964).

²⁵ S. Florens, A. Georges, G. Kotliar, O. Parcollet, Phys. Rev. B **66**, 205102 (2002).

²⁶ See, e.g., D. D. Johnson, Phys. Rev. B **38**, 12807 (1988).

²⁷ W. Nolting, W. Borgiel, Phys. Rev. B **39**, 6962 (1989).

²⁸ H. J. Vidberg and J. W. Serene, Journal of Low Temperature Physics, **29**, 179 (1977).